Finishing treatment processes for micropollutant degradation at the outlet of WWTP: Bibliometric analysis and QSPR/QSAR modeling

Yunzhi Li, Julien G. Mahy, Stéphanie D. Lambert*
Department of Chemical Engineering-Nanomaterials, Catalysis and Electrochemistry, University of Liège, Liège, Belgium

*Corresponding authors: Stephanie.Lambert@uliege.be

1. Abstract

Micropollutants are substances, both synthetic and natural, that are discharged into the environment from point and non-point sources, which typically come from wastewater treatment plants (WWTP), enter the environment with treated wastewater and may be harmful to ecosystems, wildlife, and human health. The conventional water treatment techniques find it challenging to degrade these compounds due to their high stability. Despite advanced water treatment methods, some compounds remain unremovable. The decontamination of water from non-biodegradable micropollutants has encountered obstacles, necessitating the development of advanced technologies for follow-up processing. In this review, we focus the micropollutant removal using adsorption and photocatalysis technologies, we present a bibliometric analysis on nano-adsorbents, photocatalysts, and photoelectrocatalysis (PEC) technology.

The chemical and degradation pathway diversity of micropollutants in real wastewater, experimentally determining the effectiveness of micropollutant degradation is an expensive and complex process. We propose the use nanocatatlysts to understand the quantitative relationship between the structural characteristics of micropollutants and their degradability, such as quantitative structure-property/ activity relationship (QSPR/QSAR) models. E.g., phenolic compounds with different substituents, according to the multiple linear regression (MLR) equation of the QSPR model, the degradation of phenolic compounds is greatly influenced by electronic, hydrophobic, topological, and steric properties. These QSPR models underwent strict internal and external statistical validation procedures and were trained to accurately predict the experimental degradation rate constants of the test set. We explore the potential benefits and limitations of various technologies and models for use in water treatment facilities.

Keywords: Bibliometric analysis; QSPR/QSAR model; micropollutant; photoelectrocatalytic

2. Introduction

Micropollutants (MPs), also referred to as emerging pollutants (Khan et al., 2022), are defined as synthetic and natural compounds released from point and non-point sources that end up in the aquatic environment at low concentrations (Chavoshani et al., 2020). The removal of these contaminants is challenging, as they impact ecosystems and wildlife in addition to people (Fanourakis et al., 2020; Kandie et al., 2020). Numerous studies have shown that micropollutants (MPs) have been detected in various water samples, such as pharmaceuticals, personal care products, pesticides, industrial chemicals, persistent organic pollutants, steroid hormones, artificial sweeteners, nanomaterials (Almazrouei et al., 2023; Cardenas et al., 2016; Kandie et al., 2020; Menger et al., 2021).

According to the majority of research, wastewater treatment plants (WWTP) are a significant source of MPs in water bodies (Luo et al., 2014; Menger et al., 2021). However, after the primary and secondary treatment steps of WWTP, many stable and non-biodegradable micropollutants are released into natural water systems, such as surface water, groundwater, or oceans (Klavarioti et al., 2009). Traditional WWTP can only remove biodegradable micropollutants (Terry & Summers, 2018). The decontamination of water from non-biodegradable micropollutants has encountered obstacles, necessitating the development of advanced technologies for follow-up processing.

Recent advances in nanotechnology offer new prospects for developing future water treatment systems. Some nanomaterials have shown promise in removing micropollutants more effectively in lab-scale research. Nanotechnology research has focused on adsorption, photocatalysis, and membrane filtration for water and wastewater treatment (Zhao et al., 2018). Photoelectrocatalysis combines the advantages of both photocatalysis and electrochemical oxidation. Through electric field assistance, it effectively avoids the recombination of photocatalytic photogenerated electrons and holes and increases efficiency. The problem that the powder catalyst in the photocatalytic system cannot be separated from the solution after use is also resolved. Photoelectrocatalysis is more efficient at removing non-biodegradable micropollutants than conventional electrochemical oxidation, direct photolysis, and photocatalytic processes (Daghrir et al., 2014). Photoelectrocatalytic (PEC) oxidation has begun to receive widespread attention.

Although research on adsorption, photocatalysis or photoelectrocatalysis for the removal of micropollutants has been conducted in the past few years, the majority of these investigations have not looked at their nanomaterial application in actual wastewater treatment systems (Fanourakis et al., 2020), we comprehensively bibliometric analysis, selected the most commonly used keywords. The term "wastewater treatment plant (WWTP)" only occurred once in our all-document data that was gathered. It is necessary to predict the degradation behaviour of molecules throughout the degradation process due to the diverse degradation mechanisms and the diversity of chemical characteristics of micropollutants in the photoelectrocatalytic process. Computational modelling is one possible approach to this problem. By highlighting significant molecular sites that are most pertinent to degradation, Quantitative structure – property/activity relationship (QSPR /QSAR) modelling techniques can aid in a greater understanding of reaction

pathways. QSPR models have been applied to water treatment, including adsorption, membrane filtration, coagulation, ozonation, Fenton reaction, photolysis, and photocatalysis (Awfa et al., 2021).

In this review, we give a bibliometric analysis of photoelectrocatalysis's use in practical WWTP to remove micropollutants. We focus on the advancement in nanotechnologies using adsorption and photocatalysis to decontamination water, we present a bibliometric analysis on nano-adsorbents and photocatalysts. In addition, we offer a detailed analysis of the latest advancements and application of QSPR/QSAR modelling of photocatalysis or/and photoelectrocatalysis. We use nanocatatlysts to understand the quantitative relationship between the structural characteristics of micropollutants and their degradability. Specifically, we focus on the application of photoelectrocatalytic QSPR/QSAR models to different types of micropollutants, to determine their molecular descriptors that are relevant to degradation. This enables us to predict the degradation performance of photoelectrocatalytic technology for this group of micropollutants, our focus is particularly on the use of this technology in water treatment facilities, which has not been discussed in the other articles.

3. Emerging micropollutants

3.1 Class, source, fate, effects

As seen in Table 1, micropollutants can originate from a variety of sources (such as agriculture, households, traffic networks or industries) and enter water bodies through a variety of entry paths. MPs are primarily classified as pharmaceutical pollutants and endocrine disruptors, perfluorochemicals, microplastics, pesticides and artificial sweeteners. Depending on the source, MPs transfer occurs as diffuse, such as from agricultural land use, or as point source pollution, for which WWTP are a significant source.

Over the past decade, microbial hazards to human health and environments have increased due to antibiotic resistance genes (ARGs). Table 1 shows a positive like between the horizontal transmission of ARGs mediated by class I integron (intI1) and the development of drug resistance in microorganisms in the environment. Bacitracin, sulfonamides and tetracyclines are dominant ARG types (Hu et al., 2020). Distribution is affected by interactions with other micropollutants in WWTP.

As shown in the example in Table 1, biological oxygen demand (BOD) loading and the filter medium material in biofilters have a positive effect on the degradation of pharmaceutical pollutants such as Atenolol, propranolol, venlafaxine, citalopram, metoprolol, iohexol, and diclofenac. Biological treatment is typically the main treatment method used in sewage treatment (Nord & Bester, 2020).

Microplastics can originate from a number of sources, such as the fishing industry, household grey water and WWTP. Usually, they are visible as fragments and fibres on the water's surface and in sediments (table 1). Plastic additives affect the density and source identification of microplastics. The primary constituents of microplastics include polyethylene, polypropylene,

polyester and acrylic fibres, nylon, polyethylene terephthalate and other polymers. Along with the treated wastewater, a significant amount of plastic pieces measuring between 25 μm and 50 mm are released into the environment (Edo et al., 2020).

Mecoprop and diazinon represent pesticides that often come from surface runoff and agriculture. Diazinon is also a compound with a high concentration of pesticides in urban wastewater, and its effluent concentration is also at a high level. Mecoprop is usually used as an indicator substance, mainly because it does not exist in background water, and because it is only found in wastewater (Jekel et al., 2015).

As shown in Table 1, perfluorinated compounds (PFCs) such as perfluorooctanoate (PFOA), perfluorohexanoate (PFHpA), perfluorooctane sulfonate (PFOS) and PFC conversion products, which are transported by means of suspended solids (Nguyen et al., 2012). Sediments are strongly attracted to perfluorinated compounds, which is mainly due to the long carbon chain and bulky functional groups of PFCs (Nguyen et al., 2012).

Table 1. Micropollutants (MPs), class, example, fate and their effects

Class	Example	Source	Fate	Effects	Reference
Pharmaceutical contaminants & Endocrine-disrupting chemicals (EDCs)	Antibiotic resistance genes (ARGs): tetracycline; sulfonamide; Bacitracin	Wastewater treatment plants (WWTP) and animal feces.	Class 1 integron (intI1) gene was the most important factor influencing the abundance or composition of ARGs.	Grassland and non-antibiotic micropollutants may influence the distribution of ARGs in the environment.	(Hu et al., 2020)
	Sulfamethoxazole, and bisphenol A	Industrial wastewater (chemical, pharmaceutical) plants	By increasing extracellular polymeric substances (EPS) and enzyme activity (exemple: superoxide dismutase enzyme), the micropollutants concentrations accumulated in microalgae cells also fell.	By culturing microalgae in industry wastewater sources, nutrients could be recovered. Simultaneously, Micropollutants (MPs) were able to be partially removed via cometabolism.	(Vo et al., 2020)
	Atenolol, propranolol, venlafaxine, citalopram, metoprolol, iohexol, and diclofenac	Stormwater and combined sewer overflow	Biofilters can remove pharmaceuticals from polluted water. Removal of pharmaceutical contaminants in biofilters is affected by Biochemical oxygen demand		(Nord & Bester, 2020)

			(BOD) loading and support media (materials).		
Microplastic particles	Black fibres	Greywater/river and fishing	MPs were mainly made of polyethylene terephthalate, polystyrene, and nylon.	Additives in plastic materials may affect density (buoyancy) and source identification of microplastics.	(Nematollahi et al., 2020)
	Fragments (main ingredient) and fibres	Wastewater treatment plants (WWTP)	The main polymers in wastewater are polyethylene, polypropylene, polyester and acrylic fibers.	In the range of 25 µm-50 mm, the amount of anthropogenic plastic debris released with sewage (treated) remained at 12.8 ± 6.3 particles/L.	(Edo et al., 2020)
Artificial sweetener	Acesulfame	Wastewater treatment plants (WWTP)	Acesulfame K can be used as an indicator of wastewater due to its stability and its independence from background water bodies (it is only present in wastewater)	Acesulfame K is closely related to chloride, carbamazepine and primidone.	(Jekel et al., 2015)
Pesticide	Mecoprop (Herbicides & fungicides)	Agriculture and surface runoff	Mecoprop is suggested as an indicator substance due to its widespread use and relatively high concentrations, although herbicides and fungicides might vary regionally.	Its use as an indicator of urban runoff contribution may be limited to urban areas.	(Jekel et al., 2015)
	Diazinon (Organophosphates)	Agriculture and surface runoff	Diazinon has also been the compound showing the highest concentration in the occurrence of pesticides in urban wastewaters.	Flow into the urban areas with the effluent of the sewage treatment plant.	(Rodriguez-Mozaz et al., 2015)
Perfluorochemicals (PFCs)	Perfluoroalkyl carboxylates (PFCA), especially perfluorooctanoate (PFOA), perfluorohexanoate	Sedi- mentation was the major sink for PFCs.	PFC transport is by suspended solids (SS). Sorption of PFCs (by sediments) was strongest for	The estimated annual PFC input into the reservoir was approximately 35± 12 kg y-1. .	(Nguyen et al., 2012)

	(PFHpA), perfluorooctane sulfonate (PFOS) and PFC conversion products	PFCs with long carbon chains and bulky functional groups

3.2 Ecotoxicological risk

In most cases, wastewater treatment plants (WWTP) only partially remove micropollutants occurring in the influent. Treated effluents can thus contain a complex mixture of ecotoxic pollutants.

Water resources may contain organic micropollutants, including emerging contaminants, that can have adverse effects on human health and aquatic ecosystems. Exposure to trace levels of micropollutants can lead to a reduction in the biodiversity of aquatic life and loss of ecological services and functions. Therefore, it is crucial to conduct Ecotoxicological Risk Assessments (ERA) of WWTP effluents. The standard ERA method involves predicting environmental concentration (PEC) or measuring environmental concentration (MEC) to determine each pollutant's presence and analyzing its potential effects on aquatic ecosystems using Predicted No Effect Concentration (PNEC) values. However, according to (Loiseau et al., 2012), ERA are often carried out on isolated WWTP without considering territorial ecotoxicological risks.

There is growing interest in using territory-based strategies to assess ecological risks. A technique for called Territory-based ERA was developed by (Brus & Perrodin, 2017). They used it to assess the risks of 18 wastewater treatment plants located across an area. They found that the biggest risk was posed by minor watercourses that collected wastewater from medium to small-sized WWTPs.

Several studies are now working on developing new methods to assess the toxicity and danger of combinations on a territory-wide scale. One approach is to use additive models for risk quotient (RQ) computation. The RQ value is considered safe if it is less than 1, and if it is larger than 1, it shows that there is a risk (Backhaus & Karlsson, 2014; Gosset et al., 2020). There are two main types of ERA based on the RQ calculation method: ERA of a single substance and ERA of a mixture. Studies have shown that the ERA of a mixture is more effective at revealing hidden risks than the classical single-substance approach (Backhaus & Karlsson, 2014; Gosset et al., 2020).

Sewage-receiving water bodies typically include rivers, lakes and oceans. Studies have confirmed this. The most sensitive life in rivers is fish and invertebrates, whose mixed risk quotient (MRQ) values for micropollutants in rivers (surface water and sediment) frequently surpass 1 due to polycyclic aromatic hydrocarbons (PAHs) and UV filters. (Liu et al., 2020). Second, the diversity and uniformity of zooplankton levels were significantly correlated negatively with the presence of micropollutants in the water (Liu et al., 2020).

Sloping continental margins and submarine canyons are important for understanding continental shelf/deep ocean exchange of particulate pollutants, and impacts on marine ecosystems. (Azaroff

et al., 2020) found that the highest concentrations of polycyclic aromatic hydrocarbons (PAHs), UV filters (EHMC, etc.) and muscone were measured in submarine canyon sediments far from the coast, indicating that priority and emergent pollutants raise the potential high risk to benthic animals (e.g., PAHs).

4. Bibliometric on photoelectrocatalytic oxidation and nanomaterials

4.1 Bibliometric methods and the development of academic search engines

Bibliometrics is a valuable method for analyzing and predicting research trends. The study's main concepts are summarized in keywords. As a result, we can use the co-word (co-occurrence) analysis method to identify research trends and hotspots (Zhao et al., 2018). Bibliometric reviews, in contrast to systematic literature reviews, give information on any study topic using a variety of bibliometric and bibliographic data. (Bartolacci et al., 2020). With the ability to support *ad hoc* queries and allow users to use multiple of them simultaneously in an interactive search environment, general academic search engines and databases (like Google Scholar, Baidu Scholar, and Scopus) have emerged as significant academic service providers.

Initially, the primary source for our bibliometric analysis was the Scopus database. As of July 21, 2023, a full-text search of the Scopus database for the terms "micropollutant," "photoelectrocatalytic," and "wastewater treatment plants" (WWTP) yielded only 18 unique papers.

4.2 Bibliometric on photoelectrocatalytic oxidation and WWTP

Three different search databases (Baidu Scholar, Scopus and Google Scholar) were used to find 815 research articles using the full-text search terms "micropollutants," "photoelectrocatalytic," and "wastewater treatment plants" (WWTP).

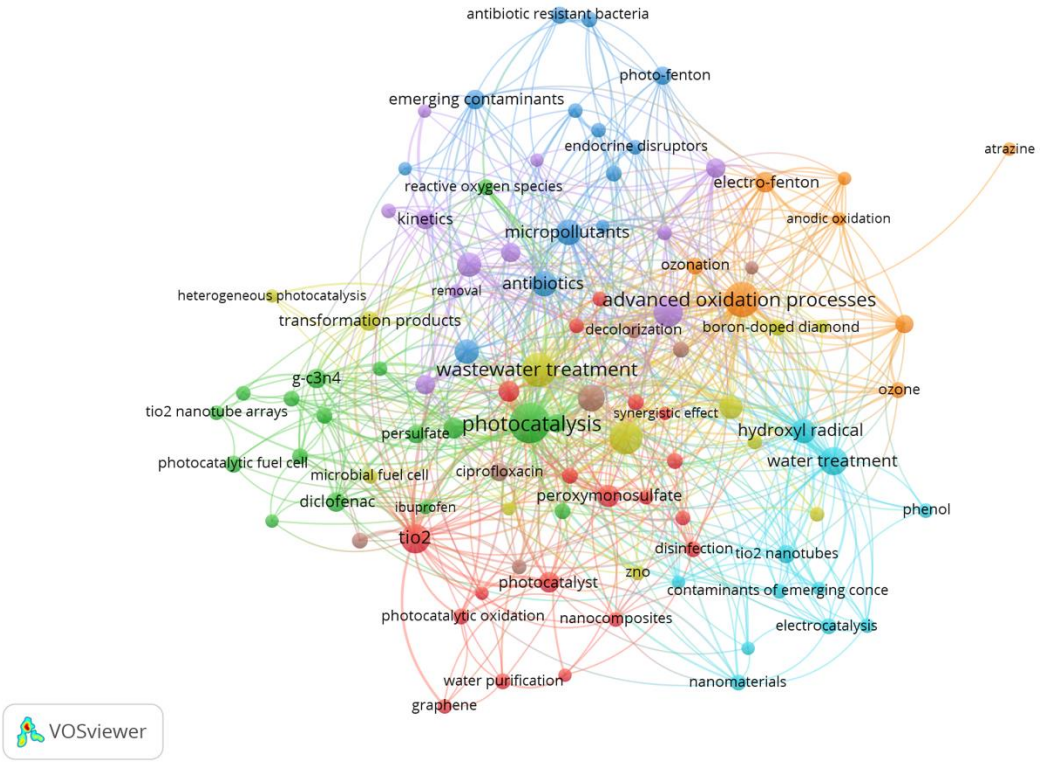

a)

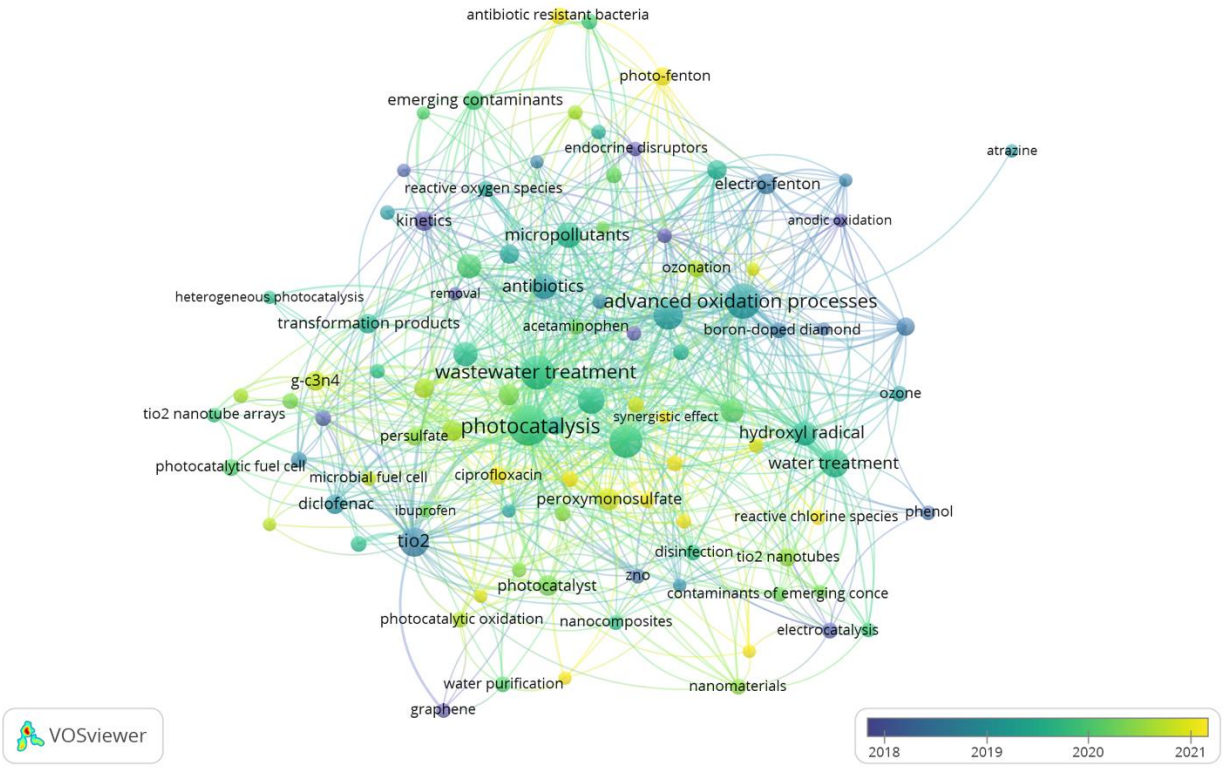

b)

Figure 1. a) Co-occurrence network visualization map and b) co-occurrence overlay visualization was created using bibliographic data obtained from full-text search that combined the keywords such as micropollutant, photoelectrocatalytic and wastewater treatment plants (WWTP). We set minimum number of keyword occurrence of 5 and found 98 out of 1827 author keyword met this threshold. Bibliographic retrieval date: July 21, 2023

We extracted 815 research papers using a comma-separated value (CSV) file so that VOSviewer (version 1.6.19) could be used for evaluation. Eight clusters with a total of 98 items (author keywords in this study) and 699 links were selected, resulting in a total link strength of 990. The supplemental file contains details regarding the links of the 98 items and the overall strength of the links (Table S1). Prior to performing VOSviewer analysis, use data cleaning techniques in OpenRefine (version 3.7.2) such as faceting, filtering, and cluster analysis to eliminate duplicate values, mistakes, and to combine singular and plural numbers and synonyms.

In the co-occurrence network visualization (Figure 1a), items are represented by circles with labels. The size of the circle and the label depends on the weight of the item. A wider circle indicates that the item (author keyword in this study) appears more frequently. However, some labels might not be visible to prevent overlapping. The colour of the circle represents the cluster

to which it belongs. Links between items are displayed by lines. The thicker the line, the more frequently the items appear together in a publication.

If two items are strongly related, they will be positioned closer to each other in the graph. An item's link and total link strength indicate the number of links it has with other items and, the total strength of the links of an item with other items., respectively. In this study, the number of co-occurrences of a given author keyword with another author keyword is represented by the link. The total strength of the co-occurrence between a given author keyword and another author keyword is represented by the total link strength.

As shown in Figure 1a, VOSviewer analysis divides it into 8 clusters. The red cluster (cluster-1); the green cluster (cluster-2); the blue cluster (cluster-3); the yellow cluster (cluster-4); the purple cluster (cluster-5); light blue (cluster-6); orange cluster (cluster-7); brown cluster (cluster-8) are shown in figure 3a. The label of items that are the largest among each cluster are those that represent the following things: photocatalysis (red cluster), TiO_2 (green cluster), antibiotics (blue cluster), wastewater treatment (yellow cluster), water treatment (purple cluster), micropollutants (light blue), advanced oxidation processes (orange cluster), and degradation (brown cluster).

Some of labels of items related to photocatalysis were photoelectrocatalysis, degradation, wastewater treatment, visible light, mechanism, degradation pathway, and electrochemical oxidation. These items are interconnected with the others through items of photocatalysis, interconnected items are located very located to each other, illustrating a hotspot in those areas.

The total link strength indicates the total strength of co-occurrence in which the two author keywords appear together. Ibuprofen (7), graphene (7), tio2 nanotube arrays (8), activated carbon (9), electro-oxidation (9), nanocomposites (11), active chlorine (12), and ZnO (13) are some of the least mentioned items (author keyword) with insufficient total link strength. Heterogeneous photocatalysis, singlet oxygen, photoelectrocatalytic degradation, and visible light photocatalysis have the lowest frequency (occurrence) and lack of links with other projects, illustrating a lack of research in those areas.

The only difference the co-occurrence overlay, and the co-occurrence network visualization is how the elements are coloured. The colour of an item corresponds to its score, with the default colour scheme ranging from blue (lowest score) to green to yellow (highest score). A colour bar is displayed in the bottom right corner of the overlay visualization. In Figure 1b's overlay visualization, colours represent the average publication year of the author keyword. The default colour scheme ranges from blue (earliest publication) to green (middle publication) to yellow (latest publication). By using overlay visualization, we can categorize items based on a time frame, which helps researchers identify possible future research areas.

Blue-coloured items appeared in the research over the last decade, including kinetics, decolourization, TiO_2, electrocatalysis, anodic oxidation, electro-Fenton, hydrogen peroxide, photodegradation, photolysis, boron-doped diamond, diclofenac.

As seen in Figure 1b, items with yellow colours include degradation mechanism, peroxymonosulfate, photo-Fenton, antibiotic-resistant bacteria, electro-oxidation, energy consumption, tetracycline, graphitic carbon nitride, ciprofloxacin, photocatalytic, synergistic effect, reactive chlorine species and escherichia coli, these areas are relatively new to photoelectrocatalytic research. These findings provide insights for further investigation.

4.3 Bibliometric on application of nanomaterials

In this section, we present the historical development and emerging trends of nanoadsorbents and photocatalysts through overlay visualizations.

a) Nanoadsorbents

We were able to retrieve bibliometric records for the years 2011 through 2022 by combining the full-text searches of keywords such as "micropollutants," "photoelectrocatalytic," and "nanoadsorbents" in the Scopus database. As of August 4, 2023, we discovered 109 relevant research articles.

After extracting 109 research papers as a CSV file, we combined synonyms and eliminated mistakes from the data using OpenRefine's data cleaning tools. The terms we gathered from 109 article titles and keywords related to nanoadsorbents are shown in Table 2. The words are broken down into four-year blocks in order to organize the development of related nanoadsorbents.

Table 2. The evolution and development of nanoadsorbents over time. (2011-2014; 2015-2018; 2019-2022)

Year	**2011-2014**	**2015-2018**	**2019-2022**
words (related to nanoadsorbents)	Activated carbon, Titania (Lim et al., 2011).	Heterogeneous (Buthiyappan et al., 2016)	Anion exchanger; Hybrid ion exchanger (Kociołek-Balawejder et al., 2019)
	Nanoparticles (Liu et al., 2019)	Core-shell nanotubes (Mushtaq et al., 2016)	
		Co-doped Fe^{3+}-$TiO_{2-x}N_x$ catalyst (Aba-Guevara et al., 2017)	Nano zirconium carbide (Zhang et al., 2019)
		ZnO/MMT nanocomposite (Khataee et al., 2017)	reduced graphene oxide (rGO) - titanium dioxide (TiO_2) nanocomposite (Zhou et al., 2019)
		Tetra-amido macrocyclic ligand (TAML)/ hydrogen peroxide (H_2O_2) (Su et al., 2018)	Ternary heterojunction MWCNT/N-TiO_2/UiO-66-NH_2 (Sun et al., 2020)
		Zero-valent iron nanofibers/reduced ultra-large graphene oxide	Cobalt doped graphene powdered sand composite

		(ZVINFs/rULGO) (Soubh et al., 2018)	(Co@graphene) (Ramasamy et al., 2020) Vanadium-titanium magnetite (Zhang et al., 2020) Yolk/shell Fe_3O_4@$MgSiO_3$ nanoreactor (Mei et al., 2020) Graphene oxide and metal organic frameworks (MOFs) co-modified composites (Tang et al., 2020) Spherical cuprous oxide nanoparticles-hybrid anion exchanger (Kociołek-Balawejder et al., 2020)
		N.A	EuxTi1-xO2-yNy/$CoFe_2O_4$ (Eu/N-doped titania coupled with cobalt ferrite) (Chen et al., 2020) Iron-porphyrin loaded biochar (Fe (TPFPP)/BC) (He et al., 2020) Graphene aerogel composite (Xiong et al., 2021) UiO-66(Zr) (Lou et al., 2021) Perylene dimiide functionalized g-C_3N_4@UiO-66 supramolecular photocatalyst (Mardiroosi et al., 2021) Porous g-C_3N_4/calcined-LDH (Yu et al., 2021) Graphene/ β-cyclodextrin Membrane (Cong et al., 2021)

		Carbon fiber cloth-UiO-66-NH_2/AgI (Qian et al., 2021) Z-scheme Bi_2O_3/TiO_2@reduced graphene oxide (Zhang et al., 2021) ZnO nanorods/Fe_3O_4-graphene oxide/metal-organic framework nanocomposite (L. Chen et al., 2021) g-C_3N_4/MOFs composite (Kamandi et al., 2021) Hydrophilic 3D N-doped carbon/CuO composites (Su et al., 2021) AQ2S@rGO nanocomposite (C.-X. Chen et al., 2021) Nickel ferrite nanoenabled graphene oxide ($NiFe_2O_4$@GO) (Bayantong et al., 2021) Cyclodextrin modified polyacrylonitrile nanofiber membranes (Chabalala et al., 2021) Ag-P_{25} Photocatalysts (Fattahi et al., 2021)
	N.A	CuS@carbon nanocomposites (Y. Chen et al., 2021) Pd,ÄìZnO/ N-doped carbon nanofibers electrode (Nada et al., 2021) CuAl-layered double hydroxide/MgO_2 nanocomposit (Aragaw et al., 2022)

		Ruthenium-modified composite electrode (Zhang et al., 2022) $CuFe_2O_4$-Ti and $CuFe_2O_4$-Ti-GO nanocomposite (Özkal, 2022) Chitin Biochar (Welter et al., 2022) An electronegative silanized β-cyclodextrin adsorbent (Duan et al., 2022) BiOI/TiO_2 flexible and hierarchical S-scheme heterojunction nanofibers membranes (Liao et al., 2022) Modified cellulose/poly(3,4-ethylenedioxythiophene) composite (Ledezma-Espinoza et al., 2022) TiO_2/carbon heterostructure fibers (Wu et al., 2022) g-C_3N_4-x/Bi/$Bi_2O_2(CO_3)$1-x(Br, I)x heterojunction (M. Wang et al., 2022) TiO_2–La 0.05%–carboxymethyl-β-cyclodextrin (CMCD) (Colpani et al., 2022) Collagen fibrous aerogel cross-linked by Fe (III) /silver nanoparticle complexes (R. Wang et al., 2022) Porous polymer layer on TiO_2-graphene (Cai et al., 2022) Composite sponge (Gao et al., 2022)
	N.A	

	Bi_2WO_6 and Bi_2O_3-ZnO heterostructure (Singh et al., 2022)
	n-n heterojunction; TiO_2/$AgBiS_2$ (Parsaei-Khomami et al., 2022)

As shown in Table 2, activated carbon, titanium, nanomaterial doping technology, carbon nanotubes, and carbon nanoparticles were the major direction in which nanoadsorbents were designed and synthesised prior to 2018. From 2018 to 2022, various nanocomposites have become emerging research directions, such as reduced graphene oxide (rGO)-titanium dioxide (TiO_2) nanocomposites; graphene oxide and metal-organic framework (MOFs) co-modified composites; AQ_2S@ rGO nanocomposites; g-C_3N_4/MOFs composite; CuAl layered double hydroxide/MgO_2 nanocomposites, and Hydrophilic 3D N-doped carbon/CuO composites.

Cyclodextrin, nanofibers, and aerogels are also important emerging directions. These findings provide insights for further investigation and can be searched using the keywords mentioned above to discover new results in the fields of photoelectrocatalysis and nanoadsorbent research.

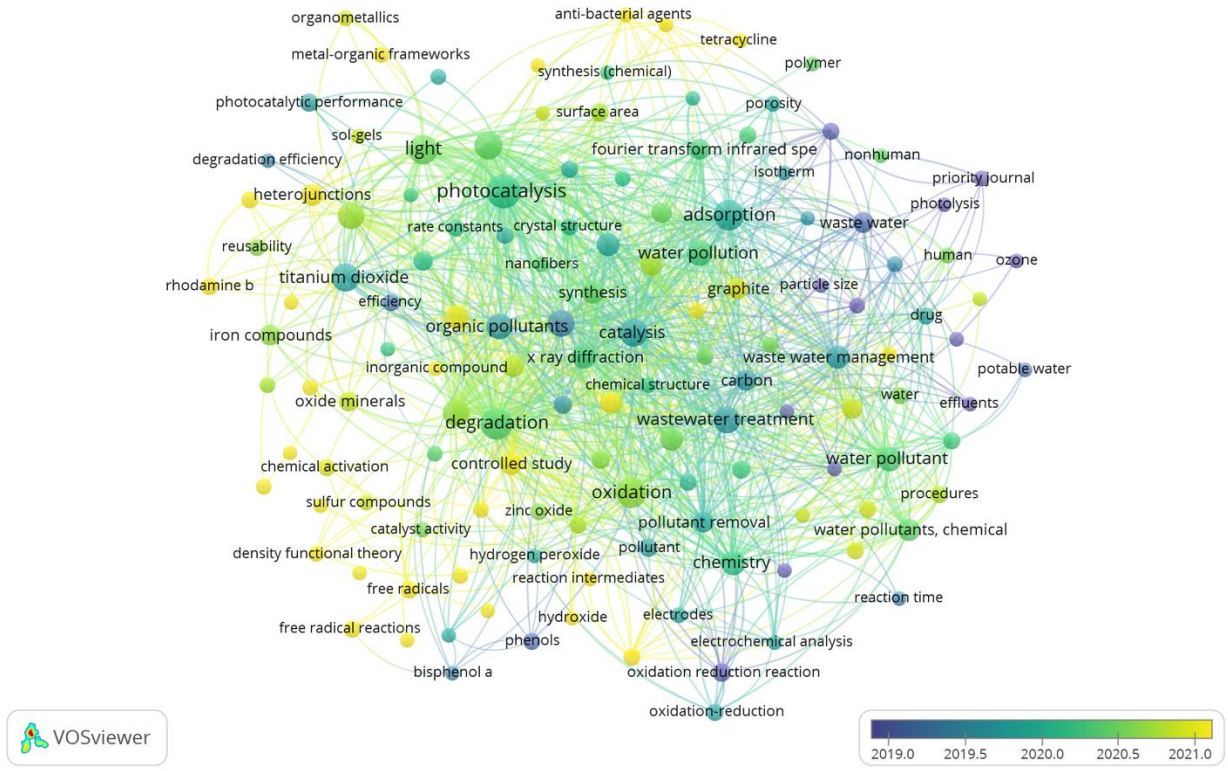

Figure 2. Co-occurrence overlay visualization was created using bibliographic data obtained from the combination full-text search of micropollutant, photoelectrocatalytic and nanoadsorbents. We set minimum number of keyword occurrence of 5, 135 out of 1603 keywords met this threshold. Bibliographic retrieval date: August 4, 2023.

Analyze all the keywords (from author and index keywords) in the CSV file using the visualization program VOSviewer (version 1.6.19). 135 items were chosen, arranged in 4 clusters with 5248 links, and given a total link strength of 10953. The supplementary file contains links and statistics on the total link strength for 135 items (Table S2).

Colours in the overlay visulization (Figure 2) represent the average year that each item was published. Bleu-coloured item has been a research hotspot in the past decade, these terms are related to "nanoadsorbents", their items labels and total link strength are as follows: catalysis (487), titanium dioxide (275), carbon (236), copper (86), titanium (185), organic pollutants (234), activated carbon (67).

Yellow-coloured items are those whose average publication year is the most recent. The item with yellow colours related to "nanoadsorbents" includes nanocomposite, graphite, inorganic compound, heterojunctions, tetracycline, anti-bacteria agents, metal-organic frameworks (MOFs), anti-infective agent. These items are recent new research directions for the design and synthesis of nanoadsorbents based on photoelectrocatalysis. Metal-organic frameworks (MOFs)

(total link strength 74), heterojunctions (total link strength 189), in particular have started to catch people's interest, and these items with low total link strength could become new research breakthrough.

b) Photocatalyst

In this section combined with the full-text search of items such as micropollutants, photoelectric catalysis, and photocatalysts, we extracted the 2011-2021 file records in the form of CSV files from the Scopus database. As of August 4, 2023, we found 296 research articles. We use OpenRefine (version 3.7.2) software to clean the duplicate or erroneous data in file records.

Use the Vosviewer (version 1.6.19) software to analyze all keywords (author and index keywords) in the CSV file. 359 items were selected from 3104 keywords. With 24868 links and 51628 total links strength. Keyword coloured yellow has the most recent average publication year. Links and total links strength information for 359 items are in the supplementary file (Table S3).

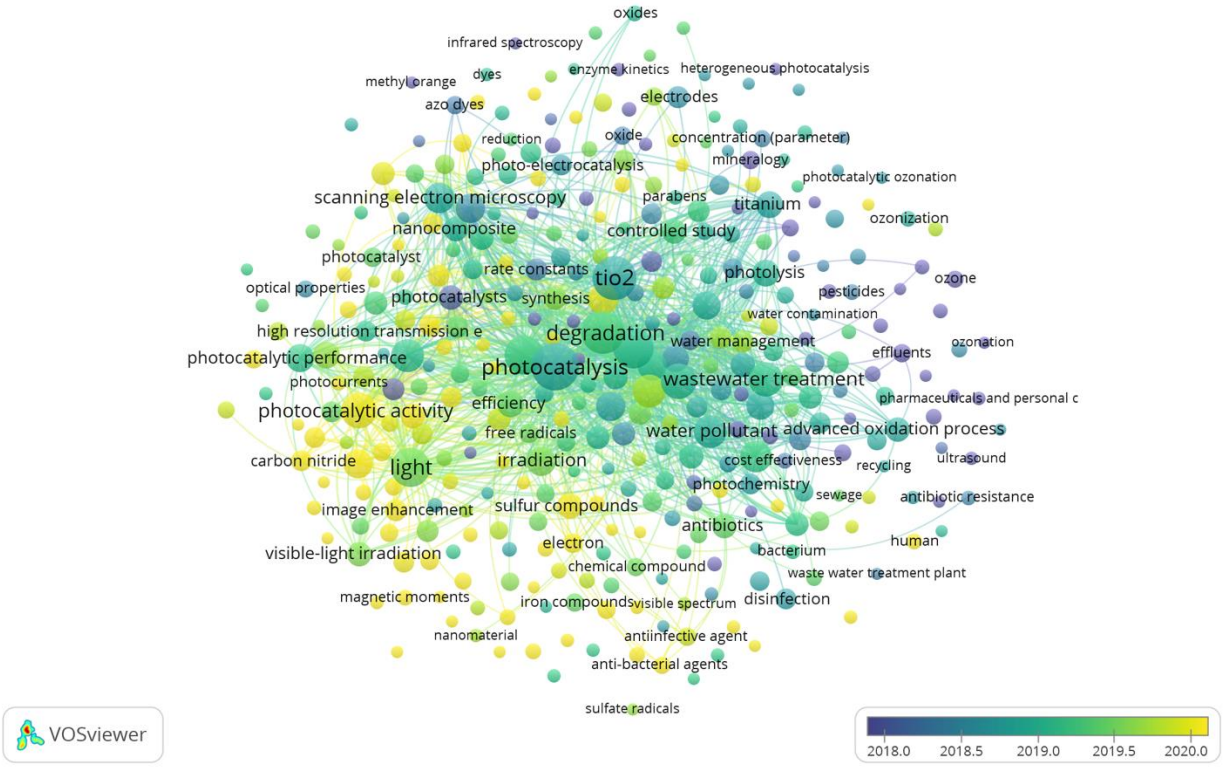

Figure 3. co-occurrence overlay visualization was created using bibliographic data obtained from the combination full-text search of micropollutant, photoelectrocatalytic and photocatalyst. We

set minimum number of keyword occurrence of 5, 359 out of 3104 keywords met the threshold. Bibliographic retrieval date: August 4, 2023

Colours indicate the average publication year of keywords. Bleu-coloured items are research in earlier publications. The items closely related to photocatalysis are as follows: TiO_2, photocatalysts, titanium, photolysis, and degradation.

Item coloured yellow has the most recent publication year. As shown in Figure 3, the yellow items are mainly clustered around the two items of "photocatalytic activity" and "light", which include Graphitic carbon nitride (g-C_3N_4), carbon nitride, heterojunctions, image enhancement, reusability, and light absorption. This may indicate that light absorption and repeatability are emerging research in photocatalysts, followed by heterojunctions, and graphitic carbon nitride nanomaterials, which help to improve light absorption and photocatalytic activity.

5. QSPR/ QSAR model predicts the therapeutic characteristics and performance of photoelectrocatalysis

Quantitative structure-property relationship (QSPR), also well as quantitative structure-activity relationship (QSAR) model approach, has proven to be useful tool for predicting treatment characteristics and performance, reducing the experimental load, and developing models based on molecular properties with minimal computational cost. These models can be applied for regulatory purposes as well (Awfa et al., 2021). However, there is a lack of exploration of methodological conditions to test the applicability of QSPR/QSAR models in real-environmentally relevant situations. This section will focus on the applicability methods and conditions of the QSPR/QSAR model in the context of real water treatment.

5.1 QSPR/QSAR principles

QSPR/QSAR is a mathematical method that link the physicochemical properties of various compounds with quantum properties derived from their molecular structures (Tian et al., 2012). The assumptions in QSPR/QSAR modelling relies on the steric, geometric, and electronic properties of a molecule that can impact its intrinsic properties. These models use measured or calculated molecular parameters of an entire group, along with appropriate mathematical and statistical methods to interpolated the unknow properties of compounds in certain group (Villaverde et al., 2018).

QSPR models are based on two main principles: (1) under similar environmental conditions, compounds with similar structures show comparable behaviour, and (2) variations in structure and composition among compounds are responsible for their behavioural differences (Chen et al., 2015).

The choice of chemical descriptors and related response variables is often the first step in the development of a QSPR/QSAR model (Awfa et al., 2021). It is possible to compute or gather molecular descriptor data from databases, literature, and experiments. Response variables can be

computed using models from previous research or by experimentation. For the purpose of running and validating the model, the data are gathered and split into two sets. The right model for the data series is then identified statistically and fitted to the curve using techniques like regression analysis, machine learning, Bayesian inference, generalized linear models, etc. The model can be used to forecast the behavior of newly discovered molecules that fall into the model's category once validation is finished.

5.2 OECD Principles for the validation of QSAR/QSPR

According to the OECD, when conducting a QSAR/QSPR study, it is essential to have 1) a well-defined endpoint, 2) an unambiguous algorithm, 3) a defined domain of applicability, 4) appropriate measures of goodness-of-fit, robustness, and predictivity, 5) a mechanistic interpretation if possible.

5.3 Validation QSAR/QSPR models

To verify and assess their influence on the performance of the QSPR/QSAR model in the application, such as water treatment, both data splitting and statistical analysis techniques can be applied (May et al., 2010). There are several methods of data splitting in the QSPR/QSAR model, including simple random sampling (SPS), convenience sampling, simple trial and error, systematic sampling, stratified sampling etc. The performance of QSPR/QSAR models is further assessed using statistical indicators, such as Root-mean-square error (RMSE), multicorrelation coefficient (R, R^2), adjusted R^2 (R_{2adj}), Fisher ratio (F), coefficient of external validation data (Q^2_{LOO}; Q^2; Q^2_{est}) and standard error (SE).

5.4 Application

In photocatalysis, light with an energy that is greater than the band gap of the semiconductor excites an electron from the valence band to the conduction band and creates an electron–hole pair. This triggers a series of reactions that lead to the degradation of pollutants. Reactive species such as hydroxyl radicals (•OH) and superoxide anion radicals ($\bullet O_2^-$)) are produced. These species are very strong and can break the bonds of stable and unreactive organic molecules, forming organic intermediates before reaching the total mineralization of contaminants. Photoelectrocatalysis combines the advantages of both photocatalysis and electrochemical oxidation. Through electric field assistance, it effectively avoids the recombination of photocatalytic photogenerated electrons and holes and improves efficiency.

As shown in Table 3, the QSPR/ QSAR model has been applied to photoelectrocatalysis, photocatalysis and involves the degradation of phenolic compounds, sulfa drugs, dyes, etc.

Prior research employed two distinct photocatalytic systems to investigate the photocatalytic degradation of ten sulfonamides (SAs): nanophase titanium dioxide plus ultraviolet ($nTiO_2$-UV) and nanophase titanium dioxide /activated carbon fiber plus UV ($nTiO_2$/ACF-UV). According to (Huang et al., 2015), QSAR studies have been conducted for two distinct systems. In the nTiO2-UV system, key molecular descriptors include the highest occupied molecular orbital (E_{homo}), the maximum values of nucleophilic attack ($f(+)_x$) and the minimum values of the most negative partial charge on a main-chain atom ($q/(C)_{min}$). In $nTiO_2$/ACF-UV system key molecular include the maximum values of •OH radical attack ($f(0)_x$) and adsorption rate constant values (K_{ad}). To develop the QSAR model, the researchers used partial least squares regression and characterized it by using multiple correlation coefficient (R^2), standard error (SE), the Fisher ratio (F), k-value test and p-value test (p). They also evaluated the developed QSAR model by using cross-validation (Q^2_{cum}) and a Williams plot. However, the researchers did not mention the data segmentation method in this study.

Huang (Huang et al., 2015) indicate that R^2 and Q^2_{ext} were above 0.5 for two different photocatalytic systems, which demonstrated that the developed models have good predictive abilities. It can be seen from the William plot that there was no outlier in the response.

(Dondapati & Chen, 2020) developed a QSPR model for prediction the of photoelectrochemical (PEC) degradation of 22 phenolic compounds using modified nanoporous TiO_2 electrodes. The model uses 5 key types of descriptors: substitute bond lipophilicity (BL S3, BLS4); radial distribution function (RDF) descriptors (55i, 45m and 30s); Global topological index (JGT); Spectral mean absolute deviation from topological distance matrix (SpMAD D), and SP-1. The radial distribution function (RDF) describes a 3-dimensional geometrical representation of a molecule. it can be interpreted as a probability of the density distribution of atoms in a spherical volume of radius r. Substitute bond lipophilicity (BL), for instance, BL S3 is a measure of hydrophobicity distribution on substituent 3. JGT is a measure of whole molecules and belongs to the Galvez topological charge indices class. The SP-1 descriptors in this study belongs to the Chi Path's descriptor class of molecular connectivity indices. The QSPR Models were validated using stringent internal and external statistical procedures, they were trained to predict the experimental degradation rate constants of the test set close to the accurate values.

The QSPR model explains the relationship between PEC degradation rate constants and important molecular descriptors, especially BL S3 and RDF. The RDF descriptor embodies contributions such as molecular density and electronic properties, BL S3 embodies hydrophobicity, and the meta-substituents with enhanced hydrophobicity are closely related to high degradation rates. Furthermore, JGT improves the predictive power during MLR modeling and the phenolic molecule with the largest JGT will be the first choice for PEC degradation. Topological descriptors related to the shape and connectivity of molecules are also crucial for improving degradation rates. Therefore, according to the MLR equation of the QSPR model, the PEC degradation of phenolic compounds is strongly dependent on electronic properties, as well as hydrophobic, topological, steric properties, etc.

According to (Ma et al., 2020), $H_3PW_{12}O_{40}$/GR/TiO_2 photocatalyst for chlorophenols and bisphenols degradation was predicted using a QSAR model. The radical distribution function-060 weighted by I-state (RDF060s), Moran autocorrelation of lag 5 weighted by mass 2D

autocorrelations (MATS5m) and K_{pre} are key molecular descriptors. QSAR model was developed by multiple linear regression (MLR) and was characterized by adjusted R^2 (R_{2adj}), coefficient of external validation data (Q^2_{LOO}), Root-mean-square error (RMSE), k value test (k_x and k_{xy}). The k values of the chosen pollutants were dependent on the structure. A QSAR model was developed with these k values. The R^2adj for the QSAR models is 0.970, which indicates that the models fit well with the training set and have good predictive abilities. Additionally, the Q^2Loo is up to 0.875, signifying that the models are statistically robust.

5.5 QSPR/QSAR model applicability domain

The applicability domain of a QSPR/QSAR model needs to be defined for it to be more meaningful. Applicability domain is mainly based on the physical and chemical properties, biological information, and structural characteristics of the compounds. By defining the appropriate applicability domain, unsuitable compound samples can be excluded before evaluation, improving the accuracy of the model. It's important to assess how broad the domain of application is, and we don't expect a useful model to only be applicable to a small space of compounds.

There are three main types of methods used to define the applicability domain: distance to model (DM), standard deviation methods, and conformal prediction methods. The DM, which is very common, uses the characteristic distance between compounds to determine whether the compound to be tested belongs to the applicability domain. Its essence is based on the similarity between the training set compounds, the test set compounds, and the new compounds to be tested. Specifically, when predicting an unknown compound, the distance between the unknown compound and all compounds in the training set is calculated. The distances of the k nearest neighbor compounds are then selected as the similarity between the compound and the training set compounds. If one of these k distances exceeds the distance of the definition domain, we consider that the compound is not in the applicability domain. It should be noted that prediction accuracy generally correlates with DM, but only on average. For example, compounds with DM in range 0.5 to 0.6 will on average have higher prediction accuracy than with DM in range of 0.6 to 0.7.

(Tetko et al., 2008) demonstrated that a DM developed using a particular set of descriptors (or one mothed) could be also used to estimate the accuracy of models developed using a different set of descriptors. The author also showed that STD-ASNN DM was effective in discriminating between molecules with low and large errors for a model based on log P and the Maximum Acceptor Superdelocalizability descriptors (Tetko et al., 2008).

Table 3. QSPR/QSAR Predictive model application in water treatment by photoelectrocatalytic / photocatalytic process. NA: not available

Treatment	Targeted contaminants	Model descriptors	Model / algorithm design	Statistical indicator value	Data splitting method	Reference
Modified nanoporous TiO_2 (Photoelectrocatalytic process)	22 phenolic compounds with varying substituents and their positional isomers (*o*, *m*, and *p*) o-CH3 m-CH3 p-CH3 m-NH2 p-NH2 m-Cl p-Cl –H m-OH p-OH o-COOH m-COOH p-COOH o-NO2 m-NO2 p-NO2 o-CHO o-NH2	21 QSPR descriptor types Important descriptors: Bond lipophilicity (BL) Radial distribution function (RDF- 55i, 45m and 30s) Global topological index (JGT) SP-1 SpMAD _ D (Spectral mean absolute deviation from topological distance matrix)	MLR	R^2adj = 0.9868 RMSE= 0.1714 FIT= 14.865 F= 151.4	NA	(Dondapati & Chen, 2020)

	o-Cl o-OH m-CHO p-CHO					
Two mechanistic models (Photocatalysis): Nanophase titanium dioxide ($nTiO_2$) plus ultraviolet (UV) $nTiO_2$/activated carbon fiber (ACF) plus UV	10 sulfonamides (SAs) sulfamethoxazole (SMZ), sulfapyridine (SPY), sulfadoxine (SFD), sulfadimidine (SM 2), sulfadimethoxine (SDM), sulfamerazine (SMI), sulfamethoxypyridazine (SMP), sulfachloropyridazine (SCP), sulfadiazine (SD), and sulfafurazole (SIZ).	9 QSAR descriptors Important descriptors: For $nTiO_2$/UV : q(C)min, Ehomo and $f(+)_x$, For $nTiO_2$/ACF: K_{ad} and $f(0)_x$.	Partial least squares regression (PLS)	For $nTiO_2$/UV : R^2= 0.923 F=16.075 SE=0.070 P=0.011 $Q^2_{(cum)}$= 0.511 For $nTiO_2$/ACF : R^2= 0.892 F=20.686 SE=0.056 P=0.004 $Q^2_{(cum)}$ = 0.829	NA	(Huang et al., 2015)
ZnO nanosheets	Methylene blue	For PL: Dislocation density,	PLS	PC (UV): R^2 calibration/	NA	(Kochnev et al., 2023)

PL-photoluminescent PC-photocatalysis		Band gap, Amount of oxygen vacancies, Cell volume For PC(UV): Zeta-potential, Defect amount, Cell volume, Vacancies to defects ratio. For PC(Vis): band gap, dark adsorption etc.		validation = 0.93/0.80, RMSEC/CV = 2.5/4.8 % PC (Vis) : R^2 calibration/ validation = 0.99/0.95 RMSEC/CV = 0.6/3.2 % PL: R^2 calibration/ validation = 0.98/0.86 RMSEC/CV = 151/459		
$H_3PW_{12}O_{40}$/GR/TiO_2 membranes (photocatalysis)	Chlorophenols (including o-chlorophenol, 2,4-dichlorophenol, 2,4,6-trichlorophenol, and pentachlorophenol) Bisphenols (such as Bisphenol A, Bisphenol AP, Bisphenol AF, and Bisphenols)	RDF 060S MATS5m	MLR	R^2_{adj}=0.970 RMSE= 0.039 Q^2_{Loo}= 0.875 K_x = 0.453 K_{xy}= 0.576	NA	(Ma et al., 2020)

6. Technological advancements

6.1 Adsorption

Adsorption on highly porous materials has proven to be an effective method for removing micropollutants. The adsorption process has been found to be superior to other technologies in terms of simplicity of design, initial costs, operation and insensitivity to toxic substrates. Activated carbons (ACs) are the most widely used adsorbent, and they are highly effective due to their high adsorption capacity (Páez et al., 2012), demonstrated for a large number of pollutants of various nature and properties (Ip et al., 2010; Páez et al., 2012). Our bibliometric analysis shows that carbon materials, specifically graphene and graphene oxide, are becoming effective adsorption materials. Porous carbon materials with high specific surface area and large pore volume, along with well-controlled morphology, are of interest to improve the process by reducing mass transport issues. The adsorption process is suitable for removing contaminants from wastewater due to the number of aromatic rings and chemical structure of these emerging pharmaceutical contaminants (Yang et al., 2008). In this process, graphene nanomaterials are dominated by π–π interactions between the aromatic rings, hydrophobic interactions, H bonding (Cortés Arriagada et al., 2013; Gao et al., 2012; Xu et al., 2012; Zhu et al., 2017).

Graphene nanomaterial and its nanocomposites are being considered above all as good candidates in water treatment due to their large surface area to volume ratio and other physiochemical properties, such as electrostatic interaction with contaminants. One of the main drawbacks of adsorption with carbon materials is the need for regeneration. Indeed, it is generally conducted by pyrolysis (thermal way) where the contaminated carbon materials are heated up to 800 °C in controlled atmosphere. This method consumes a lot of energy and time while also degrading the properties of carbon adsorbents (Lambert et al., 2009). In our group, we developed an innovative process for micropollutants from water, this process is based on adsorption with nanostructure carbons coupled with in-situ regeneration of the carbon adsorbent by combining H_2O_2 and electrophotocatalysis.

6.2 Photocatalytic

In photocatalysis, light with an energy that is greater than the band gap of the semiconductor excites an electron from the valence band to the conduction band and creates an electron−hole pair. This triggers a series of reactions that lead to the degradation of pollutants. The electron is responsible for the reduction of dissolved oxygen to form the superoxide anion ($\bullet O2^-$), while the hole helps oxidize water to create hydrogen gas and the hydroxyl radical (•OH). These products, the superoxide anion and hydroxyl radical, are oxidative agents that can break down a wide range of compounds. The process of photodegradation can occur in various ways, depending on factors such as the contaminant's chemical makeup, concentration, as well as the nanomaterial loading. As in the case of the photocatalytic degradation of ten sulfonamides (SAs) in nanophase titanium dioxide /activated carbon fiber plus UV systems. Its degradation depends on molecular descriptors including the maximum value of •OH radical attack (f(0)x) and the adsorption rate

constant value (Kad). This shows that photocatalytic efficiency is closely related to the formation rate of hydroxyl radicals.

limitation of photocatalytic material is their potential impact to the environment, particularly in the aquatic environment. The ions released during their dissolution in water can have harmful effects to the aquatic environment. Some researchers have emphasized the need for studying the toxicity of nanomaterials（such as MXene) on the environment and human health before their further water applications (Velusamy et al., 2022). It is important to understand the degradation mechanisms of photocatalysts in micropollutant and their stability in water in water treatment facilities.

7. Conclusion and perspectives

In this review, we have conducted a bibliometric analysis on nano-adsorbents, photocatalysts, and photoelectrocatalysis (PEC) technology. Our study highlights research where nanoadsorbents or photocatalysts have shown better adsorptive or photocatalytic performance in eliminating micropollutants. These nanoadsorbents or photocatalysts include materials such as graphene, cyclodextrin, nanofibers, aerogels, graphite carbon nitride, and other types of nanocomposites. Photoelectrocatalysis, degradation pathways, mechanism, visible light, and electrochemical oxidation are all connected to photocatalysis and have a significant relatedness, forming a hot study topic, as seen in the co-occurrence network visualisation diagram.

The effectiveness of micropollutants in degrading is crucial. Although numerous studies have demonstrated the great efficacy of photoelectrocatalytic and photocatalytic processes in the degradation of micropollutants, little is known about the mechanism of micropollutant degradation, particularly the degradation intermediates. Second, experimentally determining the effectiveness of micropollutant degradation is an expensive and complex process. The use of QSPR/QSAR models to forecast water treatment procedures and clarify degradation mechanisms is a promising strategy.

The outcomes showed that certain parts of the model, have excellent goodness-of-fit, robustness, and predictive capacity. Nonetheless, the performance of the QSPR/QSAR model in the water treatment application can be verified and assessed through the use of data splitting. The effectiveness of QSPR/QSAR models in water applications has not been thoroughly studied, nor have the data splitting techniques been compared in many research. Furthermore, we are unable to determine if the research using the aforementioned QSPR/QSAR models complies with the OECD's validation principles. Finally, there is little discussion on the applicability domain of the QSPR model, but it's crucial for a good model to have a wide domain.

Acknowledgements

This work has not been supported by any funding.

Contributions

All authors contributed equally to the manuscript and have read and approved the final manuscript.

References

Aba-Guevara, C. G., Medina-Ramírez, I. E., Hernández-Ramírez, A., Jáuregui-Rincón, J., Lozano-Álvarez, J. A., & Rodríguez-López, J. L. (2017). Comparison of two synthesis methods on the preparation of Fe, N-Co-doped TiO2 materials for degradation of pharmaceutical compounds under visible light. *Ceramics International*, *43*(6), 5068-5079.

Almazrouei, B., Islayem, D., Alskafi, F., Catacutan, M. K., Amna, R., Nasrat, S., Sizirici, B., & Yildiz, I. (2023). Steroid hormones in wastewater: Sources, treatments, environmental risks, and regulations. *Emerging Contaminants*, *9*(2), 100210.

Aragaw, S. G., Feysia, G. B., Gultom, N. S., Kuo, D.-H., Abdullah, H., Chen, X., & Zelekew, O. A. (2022). Synthesis of CuAl-layered double hydroxide/MgO2 nanocomposite catalyst for the degradation of organic dye under dark condition. *Applied Water Science*, *12*(6), 140.

Awfa, D., Ateia, M., Mendoza, D., & Yoshimura, C. (2021). Application of quantitative structure–property relationship predictive models to water treatment: a critical review. *ACS ES&T Water*, *1*(3), 498-517.

Azaroff, A., Miossec, C., Lanceleur, L., Guyoneaud, R., & Monperrus, M. (2020). Priority and emerging micropollutants distribution from coastal to continental slope sediments: A case study of Capbreton Submarine Canyon (North Atlantic Ocean). *Science of the Total Environment*, *703*, 135057.

Backhaus, T., & Karlsson, M. (2014). Screening level mixture risk assessment of pharmaceuticals in STP effluents. *Water research*, *49*, 157-165.

Bartolacci, F., Caputo, A., & Soverchia, M. (2020). Sustainability and financial performance of small and medium sized enterprises: A bibliometric and systematic literature review. *Business Strategy and the Environment*, *29*(3), 1297-1309.

Bayantong, A. R. B., Shih, Y.-J., Dong, C.-D., Garcia-Segura, S., & de Luna, M. D. G. (2021). Nickel ferrite nanoenabled graphene oxide (NiFe 2 O 4@ GO) as photoactive nanocomposites for water treatment. *Environmental Science and Pollution Research*, *28*, 5472-5481.

Brus, A., & Perrodin, Y. (2017). Identification, assessment and prioritization of ecotoxicological risks on the scale of a territory: Application to WWTP discharges in a geographical area located in northeast Lyon, France. *Chemosphere*, *189*, 340-348.

Buthiyappan, A., Abdul Aziz, A. R., & Wan Daud, W. M. A. (2016). Recent advances and prospects of catalytic advanced oxidation process in treating textile effluents. *Reviews in Chemical Engineering*, *32*(1), 1-47.

Cai, Z., Hu, X., He, H., Li, T., Yuan, H., Zhang, Y., Tan, B., & Wang, J. (2022). Hypercrosslinking porous polymer layers on TiO2-graphene photocatalyst: Enhanced adsorption of water pollutants for efficient degradation. *Water research*, *227*, 119341.

Cardenas, M. A. R., Ali, I., Lai, F. Y., Dawes, L., Thier, R., & Rajapakse, J. (2016). Removal of micropollutants through a biological wastewater treatment plant in a subtropical climate, Queensland-Australia. *Journal of Environmental Health Science and Engineering*, *14*, 1-10.

Chabalala, M. B., Al-Abri, M. Z., Mamba, B. B., & Nxumalo, E. N. (2021). Mechanistic aspects for the enhanced adsorption of bromophenol blue and atrazine over cyclodextrin modified polyacrylonitrile nanofiber membranes. *Chemical Engineering Research and Design*, *169*, 19-32.

Chavoshani, A., Hashemi, M., Mehdi Amin, M., & Ameta, S. C. (2020). Chapter 1 - Introduction. In A. Chavoshani, M. Hashemi, M. Mehdi Amin, & S. C. Ameta (Eds.), *Micropollutants and Challenges* (pp. 1-33). Elsevier. https://doi.org/https://doi.org/10.1016/B978-0-12-818612-1.00001-5

Chen, B., Zhang, T., Bond, T., & Gan, Y. (2015). Development of quantitative structure activity relationship (QSAR) model for disinfection byproduct (DBP) research: A review of methods and resources. *Journal of hazardous materials*, *299*, 260-279.

Chen, C.-X., Yang, S.-S., Ding, J., Wang, G.-Y., Zhong, L., Zhao, S.-Y., Zang, Y.-N., Jiang, J.-Q., Ding, L., & Zhao, Y. (2021). Non-covalent self-assembly synthesis of AQ2S@ rGO nanocomposite for the degradation of sulfadiazine under solar irradiation: The indispensable effect of chloride. *Applied Catalysis B: Environmental*, *298*, 120495.

Chen, L., Peng, J., Wang, F., Liu, D., Ma, W., Zhang, J., Hu, W., Li, N., Dramou, P., & He, H. (2021). ZnO nanorods/Fe 3 O 4-graphene oxide/metal-organic framework nanocomposite: recyclable and robust photocatalyst for degradation of pharmaceutical pollutants. *Environmental Science and Pollution Research*, *28*, 21799-21811.

Chen, Y., Su, R., Wang, F., Zhou, W., Gao, B., Yue, Q., & Li, Q. (2021). In-situ synthesis of CuS@ carbon nanocomposites and application in enhanced photo-fenton degradation of 2, 4-DCP. *Chemosphere*, *270*, 129295.

Chen, Y., Wang, X., Wang, J., & Song, Y. (2020). Photocatalytic removal of ibuprofen using euxti1-xO2-yNy/CoFe2O4 decorated on diatomaceous earth under visible light irradiation. *Journal of environmental chemical engineering*, *8*(6), 104448.

Colpani, G. L., Santos, V. F., Zeferino, R. C. F., Zanetti, M., de Mello, J. M. M., Silva, L. L., Padoin, N., Moreira, R. d. F. P. M., Fiori, M. A., & Soares, C. (2022). Propranolol hydrochloride degradation using La@ TiO2 functionalized with CMCD. *Journal of Rare Earths*, *40*(4), 579-585.

Cong, Q., Ren, M., Zhang, T., Cheng, F., & Qu, J. (2021). Graphene/β-cyclodextrin Membrane: Synthesis and Photoelectrocatalytic Degradation of Brominated Flame Retardants. *ChemistrySelect*, *6*(32), 8435-8445.

Cortés Arriagada, D., Sanhueza, L., & Wrighton, K. (2013). Removal of 4-chlorophenol using graphene, graphene oxide, and a-doped graphene (A= N, B): A computational study. *International Journal of Quantum Chemistry*, *113*(15), 1931-1939.

Daghrir, R., Drogui, P., Delegan, N., & El Khakani, M. A. (2014). Removal of chlortetracycline from spiked municipal wastewater using a photoelectrocatalytic process operated under sunlight irradiations. *Science of the Total Environment*, *466*, 300-305.

Dondapati, J. S., & Chen, A. (2020). Quantitative structure–property relationship of the photoelectrochemical oxidation of phenolic pollutants at modified nanoporous titanium oxide using supervised machine learning. *Physical Chemistry Chemical Physics*, *22*(16), 8878-8888.

Duan, C., Wang, J., Liu, Q., Zhou, Y., & Zhou, Y. (2022). Efficient removal of Salbutamol and Atenolol by an electronegative silanized β-cyclodextrin adsorbent. *Separation and Purification Technology*, *282*, 120013.

Edo, C., González-Pleiter, M., Leganés, F., Fernández-Piñas, F., & Rosal, R. (2020). Fate of microplastics in wastewater treatment plants and their environmental dispersion with effluent and sludge. *Environmental Pollution*, *259*, 113837.

Fanourakis, S. K., Peña-Bahamonde, J., Bandara, P. C., & Rodrigues, D. F. (2020). Nano-based adsorbent and photocatalyst use for pharmaceutical contaminant removal during indirect potable water reuse. *NPJ Clean Water*, *3*(1), 1.

Fattahi, A., Arlos, M. J., Bragg, L. M., Liang, R., Zhou, N., & Servos, M. R. (2021). Degradation of natural organic matter using Ag-P25 photocatalyst under continuous and periodic irradiation of 405 and 365 nm UV-LEDs. *Journal of environmental chemical engineering*, *9*(1), 104844.

Gao, B., Pan, Y., & Yang, H. (2022). Enhanced photo-Fenton degradation of fluoroquinolones in water assisted by a 3D composite sponge complexed with a S-scheme MoS2/Bi2S3/BiVO4 ternary photocatalyst. *Applied Catalysis B: Environmental*, *315*, 121580.

Gao, Y., Li, Y., Zhang, L., Huang, H., Hu, J., Shah, S. M., & Su, X. (2012). Adsorption and removal of tetracycline antibiotics from aqueous solution by graphene oxide. *Journal of Colloid and Interface Science*, *368*(1), 540-546.

Gosset, A., Polomé, P., & Perrodin, Y. (2020). Ecotoxicological risk assessment of micropollutants from treated urban wastewater effluents for watercourses at a territorial scale: Application and comparison of two approaches. *International Journal of Hygiene and Environmental Health*, *224*, 113437.

He, W., Zhu, Y., Zeng, G., Zhang, Y., Wang, Y., Zhang, M., Long, H., & Tang, W. (2020). Efficient removal of perfluorooctanoic acid by persulfate advanced oxidative degradation: inherent roles of iron-porphyrin and persistent free radicals. *Chemical Engineering Journal*, *392*, 123640.

Hu, A., Wang, H., Li, J., Mulla, S. I., Qiu, Q., Tang, L., Rashid, A., Wu, Y., Sun, Q., & Yu, C.-P. (2020). Homogeneous selection drives antibiotic resistome in two adjacent sub-watersheds, China. *Journal of hazardous materials*, *398*, 122820.

Huang, X., Feng, Y., Hu, C., Xiao, X., Yu, D., & Zou, X. (2015). Mechanistic QSAR models for interpreting degradation rates of sulfonamides in UV-photocatalysis systems. *Chemosphere*, *138*, 183-189. https://doi.org/https://doi.org/10.1016/j.chemosphere.2015.05.075

Ip, A. W. M., Barford, J. P., & McKay, G. (2010). A comparative study on the kinetics and mechanisms of removal of Reactive Black 5 by adsorption onto activated carbons and bone char. *Chemical Engineering Journal*, *157*(2), 434-442. https://doi.org/https://doi.org/10.1016/j.cej.2009.12.003

Jekel, M., Dott, W., Bergmann, A., Dünnbier, U., Gnirß, R., Haist-Gulde, B., Hamscher, G., Letzel, M., Licha, T., & Lyko, S. (2015). Selection of organic process and source indicator substances for the anthropogenically influenced water cycle. *Chemosphere*, *125*, 155-167.

Kamandi, R., Mahmoodi, N. M., & Kazemeini, M. (2021). Graphitic carbon nitride nanosheet/metal-organic framework heterostructure: Synthesis and pollutant degradation using visible light. *Materials Chemistry and Physics*, *269*, 124726.

Kandie, F. J., Krauss, M., Beckers, L.-M., Massei, R., Fillinger, U., Becker, J., Liess, M., Torto, B., & Brack, W. (2020). Occurrence and risk assessment of organic micropollutants in freshwater systems within the Lake Victoria South Basin, Kenya. *Science of the Total Environment*, *714*, 136748.

Khan, A., Ali, J., Jamil, S. U. U., Zahra, N., Tayaba, T. B., Iqbal, M. J., & Waseem, H. (2022). Chapter 22 - Removal of micropollutants. In M. Z. Hashmi, S. Wang, & Z. Ahmed (Eds.), *Environmental Micropollutants* (pp. 443-461). Elsevier. https://doi.org/https://doi.org/10.1016/B978-0-323-90555-8.00012-X

Khataee, A., Kıranşan, M., Karaca, S., & Sheydaei, M. (2017). Photocatalytic ozonation of metronidazole by synthesized zinc oxide nanoparticles immobilized on montmorillonite. *Journal of the Taiwan Institute of Chemical Engineers*, *74*, 196-204.

Klavarioti, M., Mantzavinos, D., & Kassinos, D. (2009). Removal of residual pharmaceuticals from aqueous systems by advanced oxidation processes. *Environment international*, *35*(2), 402-417.

Kochnev, N. D., Tkachenko, D. S., Kirsanov, D. O., Bobrysheva, N. P., Osmolowsky, M. G., Voznesenskiy, M. A., & Osmolovskaya, O. M. (2023). Regulation and prediction of defect-related properties in ZnO nanosheets: synthesis, morphological and structural parameters, DFT study and QSPR modelling. *Applied Surface Science*, *621*, 156828. https://doi.org/https://doi.org/10.1016/j.apsusc.2023.156828

Kociołek-Balawejder, E., Stanisławska, E., Jacukowicz-Sobala, I., Baszczuk, A., & Jasiorski, M. (2020). Deposition of spherical and bracelet-like Cu2O nanoparticles within the matrix of anion exchangers via reduction of tetrachlorocuprate anions. *Journal of environmental chemical engineering*, *8*(3), 103722.

Kociołek-Balawejder, E., Stanisławska, E., Jacukowicz-Sobala, I., & Mazur, P. (2019). Cuprite-doped macroreticular anion exchanger obtained by reduction of the Cu (OH) 2 deposit. *Journal of environmental chemical engineering*, *7*(3), 103198.

Lambert, S., Job, N., D'Souza, L., Pereira, M. F. R., Pirard, R., Heinrichs, B., Figueiredo, J. L., Pirard, J.-P., & Regalbuto, J. R. (2009). Synthesis of very highly dispersed platinum catalysts supported on carbon xerogels by the strong electrostatic adsorption method. *Journal of Catalysis*, *261*(1), 23-33.

Ledezma-Espinoza, A., Rodríguez-Quesada, L., Araya-Leitón, M., Avendaño-Soto, E. D., & Starbird-Perez, R. (2022). Modified cellulose/poly (3, 4-ethylenedioxythiophene) composite as photocatalyst for the removal of sulindac and carbamazepine from water. *Environmental Technology & Innovation*, *27*, 102483.

Liao, X., Li, T.-T., Ren, H.-T., Zhang, X., Shen, B., Lin, J.-H., & Lou, C.-W. (2022). Construction of BiOI/TiO2 flexible and hierarchical S-scheme heterojunction nanofibers membranes for visible-light-driven photocatalytic pollutants degradation. *Science of the Total Environment*, *806*, 150698.

Lim, T.-T., Yap, P.-S., Srinivasan, M., & Fane, A. G. (2011). TiO2/AC composites for synergistic adsorption-photocatalysis processes: present challenges and further developments for water treatment and reclamation. *Critical Reviews in Environmental Science and Technology*, *41*(13), 1173-1230.

Liu, B., Zhang, S. g., & Chang, C. C. (2019). Emerging pollutants—part II: treatment. *Water Environment Research*, *91*(10), 1390-1401.

Liu, J., Lu, G., Yang, H., Dang, T., & Yan, Z. (2020). Ecological impact assessment of 110 micropollutants in the Yarlung Tsangpo River on the Tibetan Plateau. *Journal of environmental management*, *262*, 110291.

Loiseau, E., Junqua, G., Roux, P., & Bellon-Maurel, V. (2012). Environmental assessment of a territory: An overview of existing tools and methods. *Journal of environmental management*, *112*, 213-225.

Lou, X., Wu, Y.-n., Kabtamu, D. M., Matović, L., Zhang, Y., Sun, X., Schott, E., Chu, W., & Li, F. (2021). Exploring UiO-66 (Zr) frameworks as nanotraps for highly efficient removal of EDTA-complexed heavy metals from water. *Journal of environmental chemical engineering*, *9*(1), 104932.

Luo, Y., Guo, W., Ngo, H. H., Nghiem, L. D., Hai, F. I., Zhang, J., Liang, S., & Wang, X. C. (2014). A review on the occurrence of micropollutants in the aquatic environment and their fate and removal during wastewater treatment. *Science of the Total Environment*, *473*, 619-641.

Ma, Y., Zhang, Y., Zhu, X., Lu, N., Li, C., Yuan, X., & Qu, J. (2020). Photocatalytic degradation and rate constant prediction of chlorophenols and bisphenols by H3PW12O40/GR/TiO2 composite membrane. *Environmental Research*, *188*, 109786. https://doi.org/https://doi.org/10.1016/j.envres.2020.109786

Mardiroosi, A., Mahjoub, A. R., Fakhri, H., & Boukherroub, R. (2021). Design and fabrication of a perylene dimiide functionalized g-C3N4@ UiO-66 supramolecular photocatalyst: Insight into enhancing the photocatalytic performance. *Journal of Molecular Structure*, *1246*, 131244.

May, R. J., Maier, H. R., & Dandy, G. C. (2010). Data splitting for artificial neural networks using SOM-based stratified sampling. *Neural Networks*, *23*(2), 283-294.

Mei, Y., Qi, Y., Li, J., Deng, X., Ma, S., Yao, T., & Wu, J. (2020). Construction of yolk/shell Fe3O4@ MgSiO3 nanoreactor for enhanced Fenton-like reaction via spatial separation of adsorption sites and activation sites. *Journal of the Taiwan Institute of Chemical Engineers*, *113*, 363-371.

Menger, F., Ahrens, L., Wiberg, K., & Gago-Ferrero, P. (2021). Suspect screening based on market data of polar halogenated micropollutants in river water affected by wastewater. *Journal of hazardous materials*, *401*, 123377.

Mushtaq, F., Asani, A., Hoop, M., Chen, X. Z., Ahmed, D., Nelson, B. J., & Pané, S. (2016). Highly efficient coaxial TiO2-PtPd Tubular nanomachines for photocatalytic water purification with multiple locomotion strategies. *Advanced Functional Materials*, *26*(38), 6995-7002.

Nada, A. A., Orimolade, B. O., El-Maghrabi, H. H., Koiki, B. A., Rivallin, M., Bekheet, M. F., Viter, R., Damberga, D., Lesage, G., & Iatsunskyi, I. (2021). Photoelectrocatalysis of paracetamol on Pd–ZnO/N-doped carbon nanofibers electrode. *Applied Materials Today*, *24*, 101129.

Nematollahi, M. J., Moore, F., Keshavarzi, B., Vogt, R. D., Saravi, H. N., & Busquets, R. (2020). Microplastic particles in sediments and waters, south of Caspian Sea: frequency, distribution, characteristics, and chemical composition. *Ecotoxicology and Environmental Safety*, *206*, 111137.

Nguyen, V. T., Gin, K. Y.-H., Reinhard, M., & Liu, C. (2012). Occurrence, fate, and fluxes of perfluorochemicals (PFCs) in an urban catchment: Marina Reservoir, Singapore. *Water Science and Technology*, *66*(11), 2439-2446.

Nord, N. B., & Bester, K. (2020). Can the removal of pharmaceuticals in biofilters be influenced by short pulses of carbon? *Science of the Total Environment*, *707*, 135901.

Özkal, C. B. (2022). Synthesis of CuFe2O4-Ti and CuFe2O4-Ti-GO nanocomposite photocatalysts using green-synthesized CuFe2O4: determination of photocatalytic activity, bacteria inactivation and antibiotic degradation potentials under visible light. *Journal of Chemical Technology & Biotechnology*, *97*(7), 1842-1859.

Páez, C. A., Contreras, M. S., Léonard, A., Blacher, S., Olivera-Fuentes, C. G., Pirard, J.-P., & Job, N. (2012). Effect of CO2 activation of carbon xerogels on the adsorption of methylene blue. *Adsorption*, *18*(3), 199-211.

Parsaei-Khomami, A., Mousavi, M., Habibi, M. M., Shirzad, K., Ghasemi, J. B., Wang, L., Yu, J., Yu, H., & Li, X. (2022). Highly efficient visible light photoelectrochemical degradation of ciprofloxacin and azo dyes by novel TiO2/AgBiS2 photoelectrocatalyst. *Solid State Sciences*, *134*, 107044.

Qian, T., Zhang, Y., Cai, J., Cao, W., Liu, T., Chen, Z., Liu, J., Li, F., & Zhang, L. (2021). Decoration of amine functionalized zirconium metal organic framework/silver iodide heterojunction on carbon fiber cloth as a filter-membrane-shaped photocatalyst for degrading antibiotics. *Journal of Colloid and Interface Science*, *603*, 582-593.

Ramasamy, B., Pratihary, N., Sekar, K., & Das, T. (2020). Cobalt promoted bifunctional graphene composite (Co@ pGSC) for heterogeneous peroxymonosulfate activation. *Chemical Engineering Journal*, *399*, 125752.

Rodriguez-Mozaz, S., Ricart, M., Köck-Schulmeyer, M., Guasch, H., Bonnineau, C., Proia, L., de Alda, M. L., Sabater, S., & Barceló, D. (2015). Pharmaceuticals and pesticides in reclaimed water: efficiency assessment of a microfiltration–reverse osmosis (MF–RO) pilot plant. *Journal of hazardous materials*, *282*, 165-173.

Singh, S., Rawat, S., Patidar, R., & Lo, S.-L. (2022). Development of Bi2WO6 and Bi2O3− ZnO heterostructure for enhanced photocatalytic mineralization of Bisphenol A. *Water Science & Technology*, *86*(12), 3248-3263.

Soubh, A. M., Baghdadi, M., Abdoli, M. A., & Aminzadeh, B. (2018). Zero-valent iron nanofibers (ZVINFs) immobilized on the surface of reduced ultra-large graphene oxide (rULGO) as a persulfate activator for treatment of landfill leachate. *Journal of environmental chemical engineering*, *6*(5), 6568-6579.

Su, H., Yu, C., Zhou, Y., Gong, L., Li, Q., Alvarez, P. J., & Long, M. (2018). Quantitative structure–activity relationship for the oxidation of aromatic organic contaminants in water by TAML/H2O2. *Water research*, *140*, 354-363.

Su, Y., Li, S., Jiang, G., Zheng, Z., Wang, C., Zhao, S., Cui, D., Liu, Y., Zhang, B., & Zhang, Z. (2021). Synergic removal of tetracycline using hydrophilic three-dimensional nitrogen-doped porous carbon embedded with copper oxide nanoparticles by coupling adsorption and photocatalytic oxidation processes. *Journal of Colloid and Interface Science*, *581*, 350-361.

Sun, J., Feng, S., & Feng, S. (2020). Hydrothermally synthesis of MWCNT/N-TiO2/UiO-66-NH2 ternary composite with enhanced photocatalytic performance for ketoprofen. *Inorganic Chemistry Communications*, *111*, 107669.

Tang, B., Dai, Y., Sun, Y., Chen, H., & Wang, Z. (2020). Graphene and MOFs co-modified composites for high adsorption capacity and photocatalytic performance to remove pollutant under both UV-and visible-light irradiation. *Journal of Solid State Chemistry*, *284*, 121215.

Terry, L. G., & Summers, R. S. (2018). Biodegradable organic matter and rapid-rate biofilter performance: A review. *Water research*, *128*, 234-245.

Tetko, I. V., Sushko, I., Pandey, A. K., Zhu, H., Tropsha, A., Papa, E., Öberg, T., Todeschini, R., Fourches, D., & Varnek, A. (2008). Critical Assessment of QSAR Models of Environmental Toxicity against Tetrahymena pyriformis: Focusing on Applicability Domain and Overfitting by Variable Selection. *Journal of Chemical Information and Modeling*, *48*(9), 1733-1746. https://doi.org/10.1021/ci800151m

Tian, M., Thind, S. S., Simko, M., Gao, F., & Chen, A. (2012). Quantitative Structure–Reactivity Study of Electrochemical Oxidation of Phenolic Compounds at the SnO2–Based Electrode. *The Journal of Physical Chemistry A*, *116*(11), 2927-2934. https://doi.org/10.1021/jp3004618

Velusamy, K., Chellam, P., Kumar, P. S., Venkatachalam, J., Periyasamy, S., & Saravanan, R. (2022). Functionalization of MXene-based nanomaterials for the treatment of micropollutants in aquatic system: A review. *Environmental Pollution*, *301*, 119034. https://doi.org/https://doi.org/10.1016/j.envpol.2022.119034

Villaverde, J. J., Sevilla-Morán, B., López-Goti, C., Alonso-Prados, J. L., & Sandín-España, P. (2018). Considerations of nano-QSAR/QSPR models for nanopesticide risk assessment within the European legislative framework. *Science of the Total Environment*, *634*, 1530-1539.

Vo, H. N. P., Ngo, H. H., Guo, W., Nguyen, K. H., Chang, S. W., Nguyen, D. D., Liu, Y., Liu, Y., Ding, A., & Bui, X. T. (2020). Micropollutants cometabolism of microalgae for wastewater remediation: effect of carbon sources to cometabolism and degradation products. *Water research*, *183*, 115974.

Wang, M., Tan, G., Ren, H., Lv, L., & Xia, A. (2022). Enhancement mechanism of full-solar-spectrum catalytic activity of g-C3N4-x/Bi/Bi2O2 (CO3) 1-x (Br, I) x heterojunction: The roles of plasma Bi and oxygen vacancies. *Chemical Engineering Journal*, *430*, 132740.

Wang, R., Zhao, P., Yu, R., Jiang, J., Liang, R., & Liu, G. (2022). Cost-efficient collagen fibrous aerogel cross-linked by Fe (III)/silver nanoparticle complexes for simultaneously degrading antibiotics, eliminating antibiotic-resistant bacteria, and adsorbing heavy metal ions from wastewater. *Separation and Purification Technology*, *303*, 122209.

Welter, N., Leichtweis, J., Silvestri, S., Sánchez, P. I. Z., Mejía, A. C. C., & Carissimi, E. (2022). Preparation of a new green composite based on chitin biochar and ZnFe2O4 for photo-Fenton degradation of Rhodamine B. *Journal of Alloys and Compounds*, *901*, 163758.

Wu, J.-C., Chuang, Y.-H., Liou, S. Y. H., Li, Q., & Hou, C.-H. (2022). In situ engineering of highly conductive TiO2/carbon heterostructure fibers for enhanced electrocatalytic degradation of water pollutants. *Journal of hazardous materials*, *429*, 128328.

Xiong, T., Ye, Y., Luo, B., Shen, L., Wang, D., Fan, M., & Gong, Z. (2021). Facile fabrication of 3D TiO2-graphene aerogel composite with enhanced adsorption and solar light-driven photocatalytic activity. *Ceramics International*, *47*(10), 14290-14300.

Xu, J., Wang, L., & Zhu, Y. (2012). Decontamination of bisphenol A from aqueous solution by graphene adsorption. *Langmuir*, *28*(22), 8418-8425.

Yang, L., Liya, E. Y., & Ray, M. B. (2008). Degradation of paracetamol in aqueous solutions by TiO2 photocatalysis. *Water research*, *42*(13), 3480-3488.

Yu, Y., Chen, D., Xu, W., Fang, J., Sun, J., Liu, Z., Chen, Y., Liang, Y., & Fang, Z. (2021). Synergistic adsorption-photocatalytic degradation of different antibiotics in seawater by a porous g-C3N4/calcined-LDH and its application in synthetic mariculture wastewater. *Journal of hazardous materials*, *416*, 126183.

Zhang, B., Ji, J., Liu, X., Li, C., Yuan, M., Yu, J., & Ma, Y. (2019). Rapid adsorption and enhanced removal of emodin and physcion by nano zirconium carbide. *Science of the Total Environment*, *647*, 57-65.

Zhang, J., Wu, H., Zhang, D., Zhang, L., & Zhu, C. (2022). Preparation of a ruthenium-modified composite electrode and evaluation of the degradation process and degradation mechanism of doxycycline at this electrode. *Journal of Water Process Engineering*, *48*, 102904.

Zhang, W., Tang, G., Yan, J., Zhao, L., Zhou, X., Wang, H., Feng, Y., Guo, Y., Wu, J., & Chen, W. (2020). The decolorization of methyl orange by persulfate activated with natural vanadium-titanium magnetite. *Applied Surface Science*, *509*, 144886.

Zhang, Y., Yu, H., Li, S., Wang, L., Huang, F., Guan, R., Li, J., Jiao, Y., & Sun, J. (2021). Rapidly degradation of di-(2-ethylhexyl) phthalate by Z-scheme Bi2O3/TiO2@ reduced graphene oxide driven by simulated solar radiation. *Chemosphere*, *272*, 129631.

Zhao, L., Deng, J., Sun, P., Liu, J., Ji, Y., Nakada, N., Qiao, Z., Tanaka, H., & Yang, Y. (2018). Nanomaterials for treating emerging contaminants in water by adsorption and photocatalysis: Systematic review and bibliometric analysis. *Science of the Total Environment*, *627*, 1253-1263.

Zhou, X., Zhou, S., Ma, F., & Xu, Y. (2019). Synergistic effects and kinetics of rGO-modified TiO2 nanocomposite on adsorption and photocatalytic degradation of humic acid. *Journal of environmental management*, *235*, 293-302.

Zhu, S., Liu, Y.-g., Liu, S.-b., Zeng, G.-m., Jiang, L.-h., Tan, X.-f., Zhou, L., Zeng, W., Li, T.-t., & Yang, C.-p. (2017). Adsorption of emerging contaminant metformin using graphene oxide. *Chemosphere*, *179*, 20-28.